Int. J. Electrochem. Sci., 11 **(2016)** 4526 – 4538, doi: 10.20964/2016.06.20

International Journal of
ELECTROCHEMICAL
SCIENCE
www.electrochemsci.org

Synthesis, Characterization and Electrical Conductivity of Polyaniline-$Mn_{0.8}Zn_{0.2}Fe_2O_4$ Nano-composites

M.A. Gabal[1,*], *M.A. Hussein*[1,2], *A.A. Hermas*[2]

[1]Chemistry department, Faculty of Science, King Abdulaziz University, P.O. Box 80203 Jeddah 21589, KSA
[2]Chemistry Department, Faculty of Science, Assiut University, Assiut 71516, Egypt
[*]E-mail: mgabalabdonada@yahoo.com

Received: 2 March 2016 / *Accepted:* 3 April 2016 / *Published:* 4 May 2016

The polyaniline/$Mn_{0.8}Zn_{0.2}Fe_2O_4$ (PANI/MZFO) nano-composites, with different ferrite contents (10, 20 and 30 wt%), were prepared via in situ polymerization technique using aniline and MZFO prepared using citrate auto-combustion route. The produced composites were characterized using X-ray diffraction (XRD), Fourier transform infrared (FT-IR), thermogravimetry (TG), transmission electron microscopy (TEM) techniques. The effect of compositional variation on the electromagnetic properties of PANI was measured using vibrating sample magnetometer (VSM) and ac-conductivity as a function of temperature. The results of XRD and FT-IR indicated an interfacial interaction between PANI and MZFO crystallites. TEM images showed that MZFO particles are embedded in the PANI matrix and formed core-shell structure. TG curves exhibited an increase in the thermal stability of PANI with the addition of MZFO. The hysteresis measurements indicate an improvement in the magnetic properties by the addition of ferrite. The conductivity measurements confirmed the interaction between PANI and MZFO and showed a change from metallic to semi-conducting properties by the addition of MZFO.

Keywords: Conducting polymer; $Mn_{0.8}Zn_{0.2}Fe_2O_4$; Thermal stability; Conductivity; VSM.

1. INTRODUCTION

Because of their potential applications in various fields, conducting polymers have attracted the interest of many researchers as they combine the mechanical and chemical properties of polymers with the electronic properties of metals and semiconductors [1]. They can be used in electromagnetic interference (EMI) shielding, rechargeable batteries, sensors, corrosion protection, coatings, microwave absorption, etc [2].

Among conducting polymers, polyaniline (PANI) is considered as the most important member owing to its unique electrical–electrochemical properties, high environmental stability, low cost, facile

polymerization combined with high levels of electronic conductivity as well as thermoelectric and optical properties [3,4]. It can be prepared either chemically or electrochemically. The most reasonable method for its mass production is through oxidative polymerization using ammonium peroxodisulfate as an oxidant [5].

Recently, considerable attentions were focused to develop the PANI properties through the fabrication of nano-composites by incorporating inorganic nanoparticles in the PANI structure [6-9]. Using this process, a combination of the properties that are difficult to obtain with the individual components could be attained. An example for these improvements is the incorporation of some inorganic magnetic materials such as ferrites in the structure of PANI to produce new materials of magneto-conducting polymers with unique properties [10-18].

The incorporation of ferrites in the PANI structure can lead to an increase in its thermal stability [11], however, it could affect its electrical conductivity [19,20]. On the other hand, the electromagnetic properties of the PANI/ferrites could be successfully improved and tailored by controlling the addition of the ferrites [21,22] or in some cases through using different preparation methods [16-18]. These composites have many applications in many fields such as information storage, nonlinear optics, magnetic refrigeration, magnetic mediated hyperthermia, separation and purification of biomolecules, drug delivery, sensors, electrode materials in supercapacitors, etc. [17].

Lee et al. [18] synthesized $Mn_{1-x}Zn_xFe_2O_4$–polyaniline core–shell structure through aniline polymerization in the presence of surfactant and ferrites, prepared via glycine combustion route. The core–shell structure of ferrite–polyaniline composites was estimated using SEM and TEM techniques and was fortified using XRD measurements. The conductivity of the ferrites core materials showed an obvious increase on coating while magnetic measurements indicated a gradual decrease with increasing the amount of polyaniline.

Babayan et al. [17] deposited polyaniline film on the surface of manganese–zinc ferrite during in-situ polymerization process. The coercivity as well as thermomagnetic stability is observed to increase compared with those of bare ferrite or its mixed composite with polyaniline.

In the present study, an approach to synthesize PANI/$Mn_{0.8}Zn_{0.2}Fe_2O_4$ nano-composites, with different ferrite contents (10, 20 and 30 wt%), by in situ polymerization of aniline was reported. The entire ferrite was prepared using citrate sol-gel auto-combustion method. The structural, morphological, thermal, magnetic and electrical properties of the obtained composites were investigated using X-ray diffraction (XRD), Fourier transform infrared (FT-IR), thermogravimetry (TG), transmission electron microscopy (TEM), vibrating sample magnetometery (VSM) and conductivity measurements. The effect of incorporating Mn-Zn ferrite in the PANI structure as well as the effect of composition on the different properties was investigated and discussed.

2. EXPERIMENTAL PROCEDURES

2.1. Preparation of $Mn_{0.8}Zn_{0.2}Fe_2O_4$ ferrite

Nano-sized $Mn_{0.8}Zn_{0.2}Fe_2O_4$ (MZFO) was prepared using citrate sol–gel auto-combustion method [23]. Stoichiometric amounts of analytical reagents (BDH) $Mn(NO_3)_2{\cdot}4H_2O$, $Zn(NO_3)_2{\cdot}6H_2O$,

$Fe(NO_3)_2 \cdot 9H_2O$ and citric acid; $C_6H_8O_7.H_2O$ were dissolved in deionized water in 1:1 mole ratio. After adjusting the pH of solution to about 7, it was heated at 80ºC until transform into gel. With further heating and after evaporation of the entire water, the dried gel was ignited and this auto-combustion reaction propagated rapidly until all the gel was burnt out completely with the formation of MZFO through the solid-state diffusion process [24]. The combustion reaction can be written as follows [23]:

$0.8Mn(NO_3)_2.4\ H_2O + 0.2Zn(NO_3)_2.6\ H_2O + 2Fe(NO_3)_3.9\ H_2O + C_6H_8O_7.\ H_2O \rightarrow Mn_{0.8}Zn_{0.2}Fe_2O_4 + 4N_2 + 6CO_2 + 28.4H_2O + 5O_2$

2.2. Preparation of pure PANI

Pure PANI was prepared using polymerization method described in [25]. In this procedure, 1 ml of aniline monomer was dissolved into 35 ml 0.5 mol/L H_3PO_4 solution and sonicated for 30 min. 2.78 g of the oxidant; ammonium persulfate dissolved in 20 ml 0.5 mol/L H_3PO_4 solution was added dropwisly during constant stirring. The stirring was continued at 0^oC under nitrogen atmosphere for 24 h. The obtained green precipitate was filtered, washed with deionized water and ethanol then dried under vacuum at 50^oC for 24 h.

2.3. Preparation of PANI/ MZFO nano-composites

PANI/MZFO nano-composites were prepared through a simple in situ polymerization method of PANI in the presence of different percentage of MZFO nanoparticles (10, 20 and 30 wt%) with respect to the aniline monomer. In a typical procedure, an appropriate amount of MZFO was dispersed in aniline monomer and the same polymerization procedure was followed as mentioned above. An expected polymerization process is illustrated in Fig. 1.

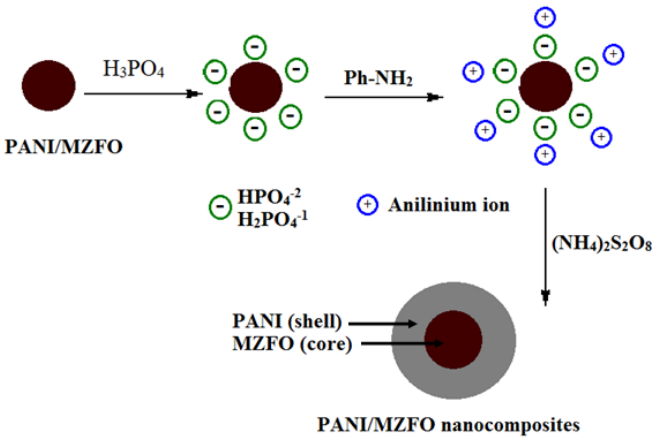

Figure 1. An illustration of the expected in-situ polymerization process for PANI/MZFO nano-composite.

The surface of the entire ferrite under the present acidic conditions is positively charged [26]. The negatively charged $H_2PO_4^-$ and HPO_4^{--} ions are then adsorbed on the ferrite surface in order to compensate the charges [25]. At the same time, the aniline monomers under the present acidic conditions are converted to cationic anilinium ions, which interact electrostatically with the adsorbed phosphate anions. Finally, the $(NH_4)_2S_2O_8$ oxidant polymerize the adsorbed anilinium ions on the ferrite surface to produce PANI/MZFO nano-composite.

2.4. Instrumentation

XRD patterns were collected on a Bruker axs D8 diffractometer with Cu-Kα radiation source (λ = 1.5405 Å) operated at 40 kV and 25 mA.

FT-IR spectra were recorded on Shimadzu-8300 spectrometer in the range of 4000–200 cm^{-1} with a resolution of 2 cm^{-1}.

TEM images were obtained using a JEOL (JEM-1011 electron microscopy) operated at an accelerating voltage of 100 kV.

Differential thermal analysis-thermogravimetry (DTA-TG) measurements were carried out using a Perkin Elmer thermal analyzer at a heating rate of 5^oC/min and a flow rate of 40 ml/min in air atmosphere up to 700^oC.

The magnetic measurements were carried out at room temperature using a vibrating sample magnetometer (VSM-9600M) with a maximum magnetic field up to 5 kOe.

In the electrical measurements, the powders were pressed into pellets of 1 cm diameter and about 1 mm thickness using a pressure of 2 tons cm^{-2}. The pellets were coated by silver paste on both sides and tested for ohmic contact. A Hioki LCR high tester 3531, using the two-probe method, as a function of frequency (100 Hz – 5 MHz) and temperature up to 823 K., measured the dielectric properties as well as the conductivity.

3. RESULTS AND DISCUSSION

3.1. X-ray diffraction

Fig.2 showed X-ray diffraction patterns of pure PANI, pure MZFO as well as PANI/MZFO nano-composites with different compositions. The well-resolved diffraction peaks corresponding to (111), (220), (311), (400), (422), (511) and (440) reflection planes confirmed the formation of single-phase cubic ferrite (JCPDS card No. 74-2399). The broadness of the diffraction peaks suggested the nano-sized characteristics of the entire ferrite. The average crystal size calculated according to Scherrer's equation is amounted to about 28 nm. XRD pattern of PANI exhibited two broad diffraction peaks at about 2θ = 20.8° and 25.5°. These peaks can be attributed to the periodicity parallel and perpendicular to the polymer chains, respectively [27].

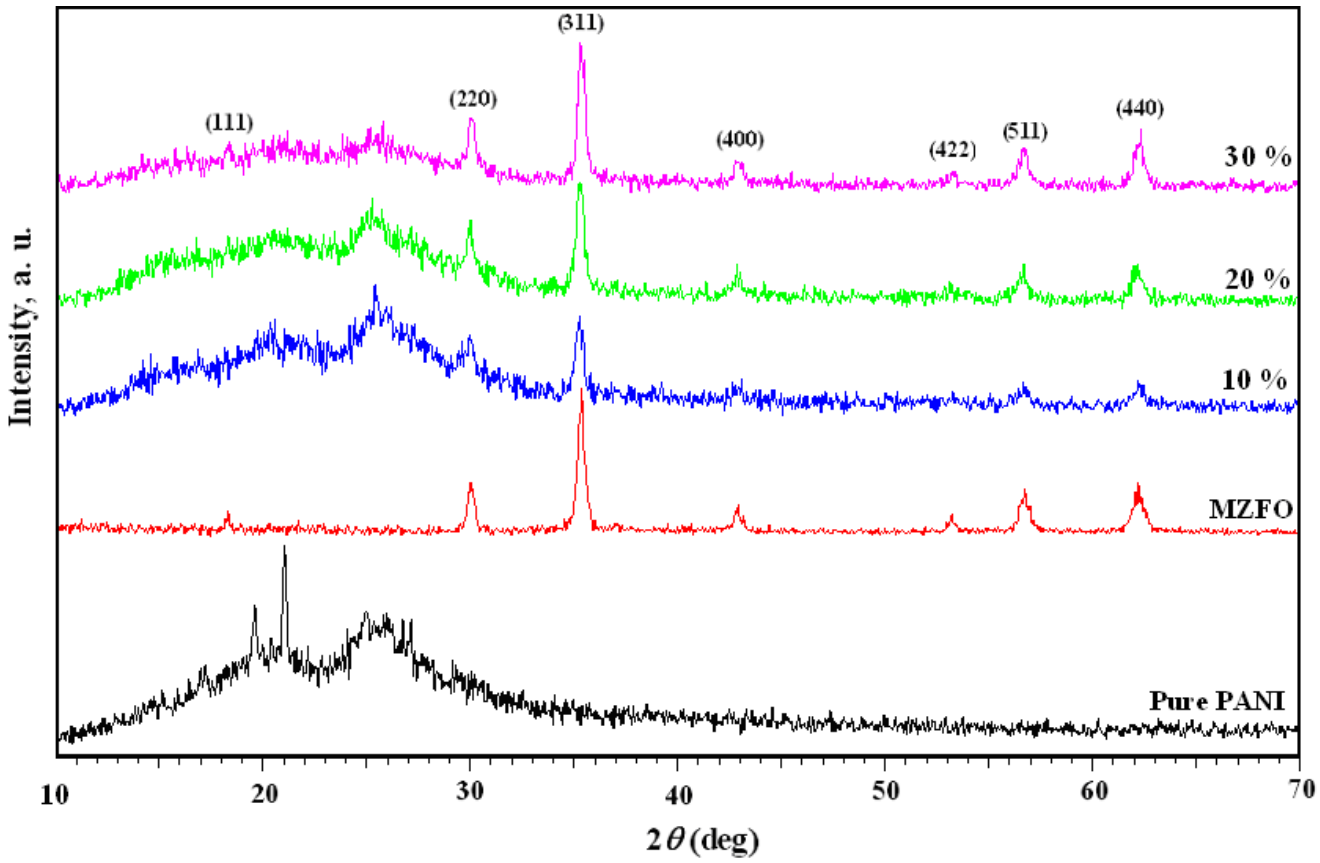

Figure 2. XRD patterns of pure components and nano-composites with different compositions.

XRD patterns of PANI/MZFO with different compositions (10-30 wt%) showed only the superposition of the diffraction peaks corresponding to polyaniline and the entire ferrite without any indication for the presence of new phases. This indicates the formation of PANI/MZFO nano-composites. The crystallite sizes (L) calculated according to Scherrer's equation for the different compositions are reported in Table 1.

Table 1. Crystallite sizes and magnetic data of the investigated samples.

Sample	L, nm	M_S	H_C
MZFO	28	50.1	74.9
10 %	13	2.0	91.7
20 %	16	3.2	92.1
30 %	18	5.2	88.2

3.2. FT-IR spectra

FT-IR spectra of PANI, MZFO and PANI/MZFO nano-composite (30 %) are illustrated in Fig. 3. The spectrum of the pure PANI exhibited intensive bands at 1565, 1480, 1294, 1235, 1079 and 789 cm^{-1} which describes PANI structure [28,29]. The bands at 1565 and 1480 cm^{-1} are assigned to C=C stretching vibration of quinoid (Q) and benzenoid rings, respectively indicating the oxidation of emeraldine form of PANI. The bands appeared at 1294, 1235 cm^{-1} are attributed to C-N stretching of secondary aromatic amine. The bands positions at 1170-1010 and 789 cm^{-1} reflected the aromatic C-H in-plane bending mode and out-of-plane deformation of C-H in 1,4-distributed benzene ring, respectively.

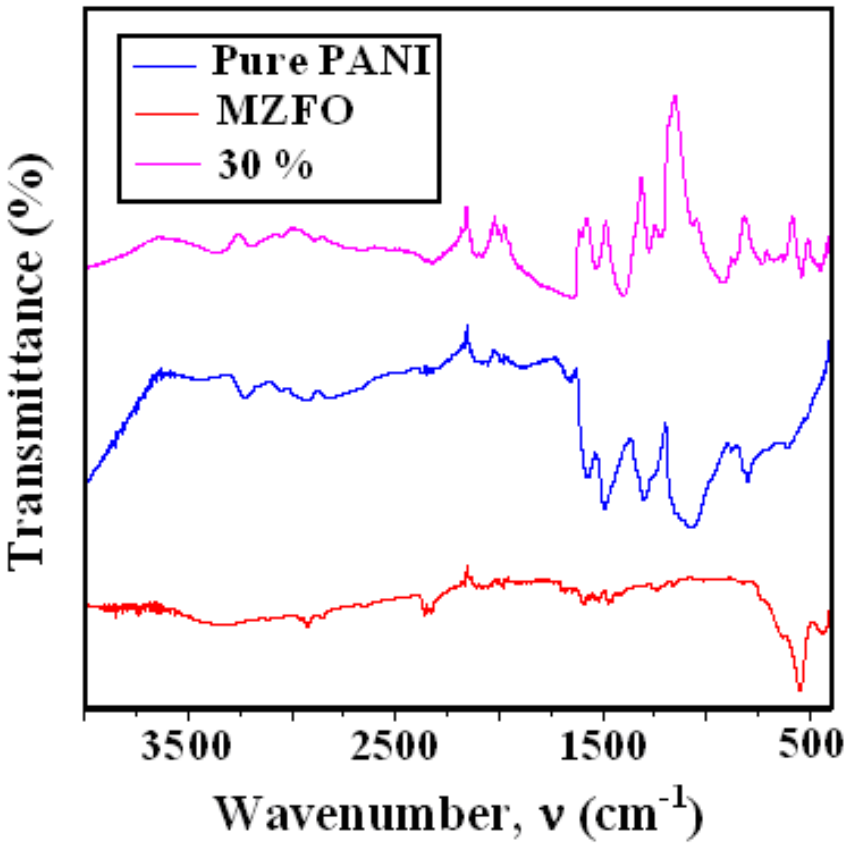

Figure 3. FT-IR spectra of pure components and PANI/MZFO nano-composite (30%).

FT-IR spectrum of MZFO showed only two bands at 548 and 436 cm^{-1}. According to Waldron [30], these band are considered as the characteristic one of spinel ferrite. The higher frequency band is assigned to the stretching vibration of Fe^{3+} in the tetrahedral sites whereas, the lower frequency one is attributed to stretching vibration in the octahedral sites. The spectrum of PANI/MZFO composite showed a combination of the two spectra attributed to the pure components. The obvious red shift in the characteristic bands of PANI can be attributed to the interaction between PANI and MZFO, which leads to weaken N-H, C-N and N-Q-N bonds [29].

3.3. TEM

The morphology and particle size of pure polyaniline, manganese-zinc ferrite and PANI/MZFO composite (20 wt%) identified by TEM are illustrated in Fig. 4. It is clear that PANI exhibited fibrous shape with average thickness of about 300 nm and length of about 1 μm. TEM image of crystalline MZFO indicated semi-spherical agglomerated particles with an average size of 22 nm, which agrees well with that estimated using XRD measurements. This agglomeration behavior can be due to the magnetic dipole interaction exerted between magnetically ferrite particles.

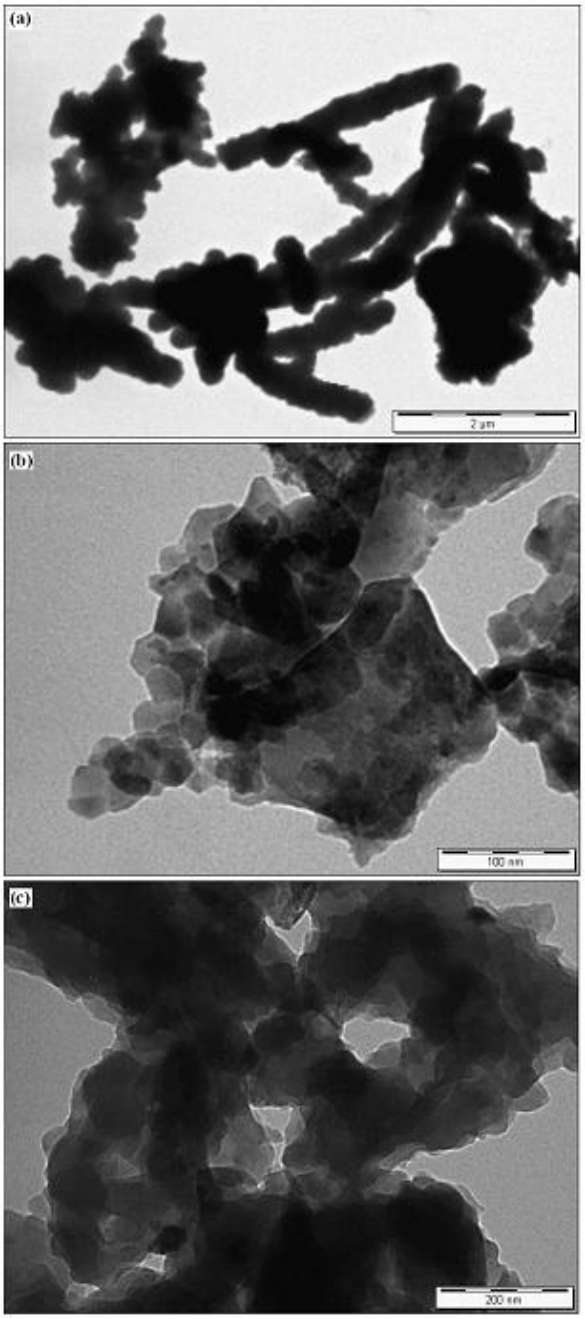

Figure 4. TEM image. (a) Pure PANI, (b) MZFO and (c) PANI/MZFO nano-composite (20%).

The image corresponding to PANI/MZFO composite showed that MZFO particles are embedded in the PANI matrix and formed core-shell structure. Owing to the different electron beam penetrability, the dark core is attributed to the ferrite particles whereas, the light colored shell are assigned to the PANI matrix [31]. The PANI matrix was irregularly polymerized on the ferrite surface and at the same time, the agglomeration of the ferrite particles is obviously reduced. This indicates the suitability of PANI matrix to the dispersion and stabilization of ferrites.

3.4. TG behavior and thermal stability

TG curves of the entire investigated samples (Fig. 5) were compared to investigate the effect of ferrite content on the thermal stability of polyaniline. The first weight loss observed for PA can be ascribed to the dehydration and HCl loss [32].

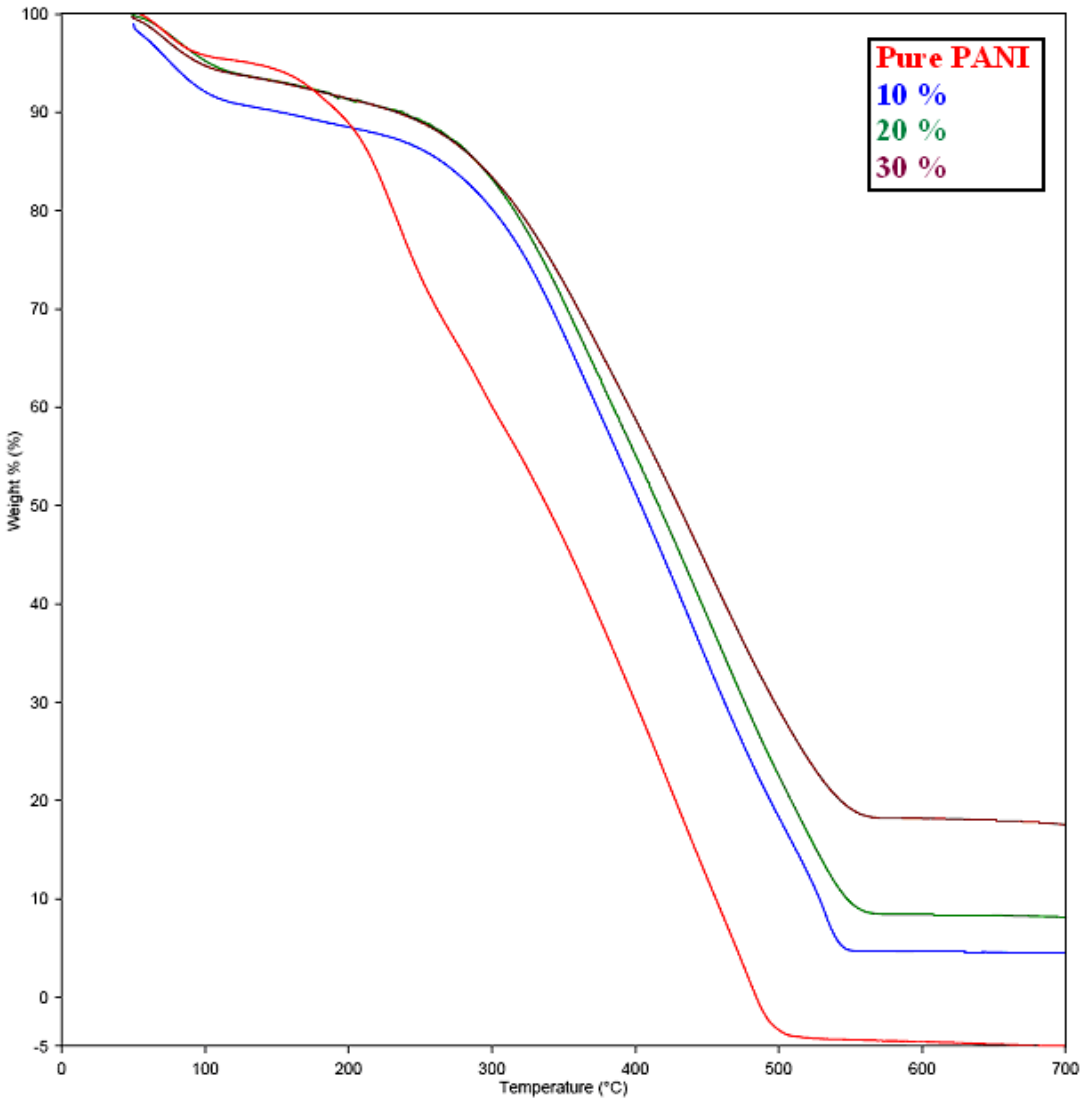

Figure 5. TG curves for Pure PANI and PANI/MZFO nano-composites with different compositions. Heating rate = 5ºC min^{-1}.

The further weight loss obtained which can be divided into two ranges: the first up to 320^{o}C can be attributed to the volatilization of chloride ions compensating the positive characteristics of PANI chains while the second at higher temperature up to 510^{o}C, which can be assigned to the decomposition of molecular PANI chains [33].

From the figure, it is clear that, the addition of ferrite increases the thermal stability of PA, which suggests the presence of intermolecular interactions between MZFO and PANI. The 50 % weight loss is observed at 338^{o}C for pure PANI whereas appeared at 435, 450 and 488^{o}C for the composites with increasing ferrite content, respectively. This behavior enhances the use of PANI/MZFO as a magnetic conducting polymer in high temperature applications.

The obvious change in the weight loss with increasing ferrite content can be due to the change in the compositional ratio by the addition of thermally stable MZFO.

3.5. Magnetic properties

The magnetic hysteresis loops of the pure MZFO as well as its composites with PANI are illustrated in Fig. 6.

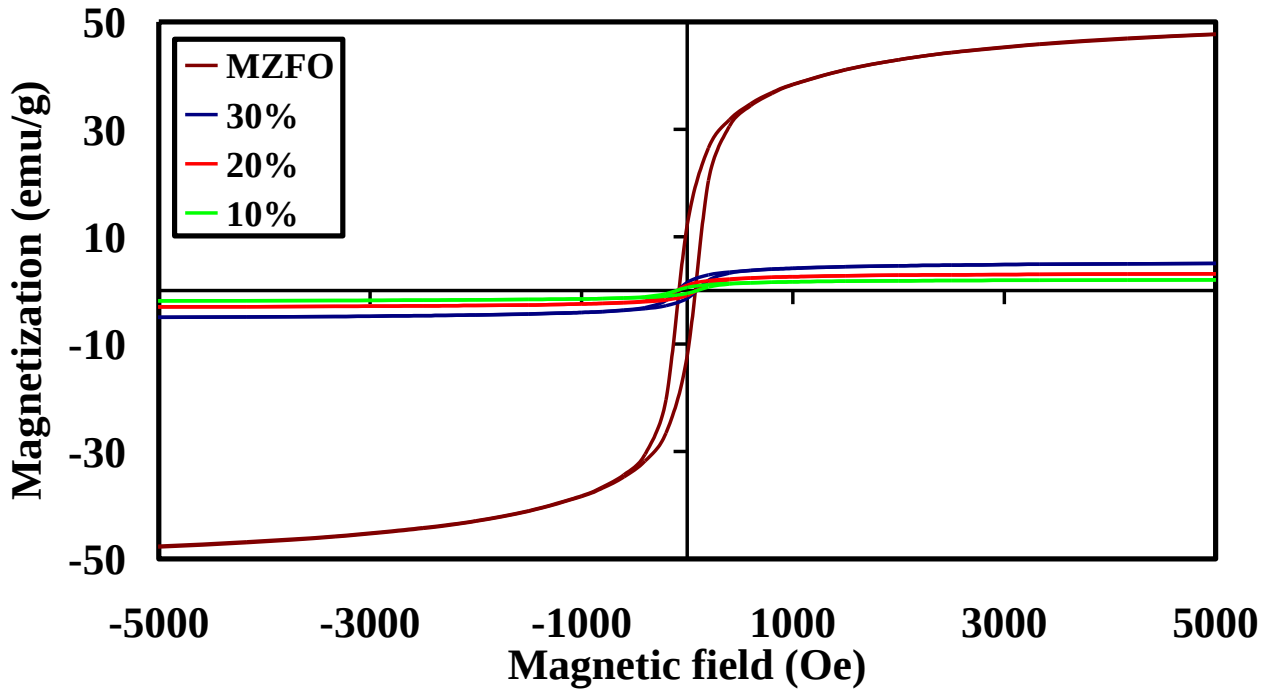

Figure 6. Hysteresis loops of MZFO and nano-composites with different compositions.

Magnetic parameters such as saturation magnetization (M_s) and coercivity (H_c) are reported in Table 1. From the figure, it is evident that, MZFO exhibit soft ferromagnetic characteristics with saturation magnetization value of 50.1 emu/g.

The composite nanoparticles with 30% of nano-ferrite showed an obvious decrease in the magnetization indicating the incorporation of the entire ferrite in core-shell structure with PANI matrix. In this structure, the PANI coating lower the magnetic super exchange interaction among Fe^{3+} ions in the core material. By increasing PANI content (the samples with 20 and 10 wt% nano-ferrite), the magnetization values (Table 1) are observed to decrease directly. This behavior can be discussed based on the shielding action of nonmagnetic PANI-shell.

The relatively high coercivity values of the nano-composites (88-92 kOe) illustrate the aggregation characteristics of the particles as revealed from TEM study. On the other hand, the improvement of the PANI magnetic properties by addition of entire ferrite can be of important impact in magnetic conducting polymer applications.

3.6. Electrical properties

The frequency dependent conductivity for disordered materials such as polymers can be due to interfacial polarization at contacts and grain boundaries of the sample [34].

Fig. 7 shows the frequency dependence of $\ln\sigma_{ac}$ conductivity as a function of temperature for pure PANI, Pure MZFO and PANI/MZFO composites with different compositions. The conductivity of all the studied samples is observed to be frequency as well as temperature dependent.

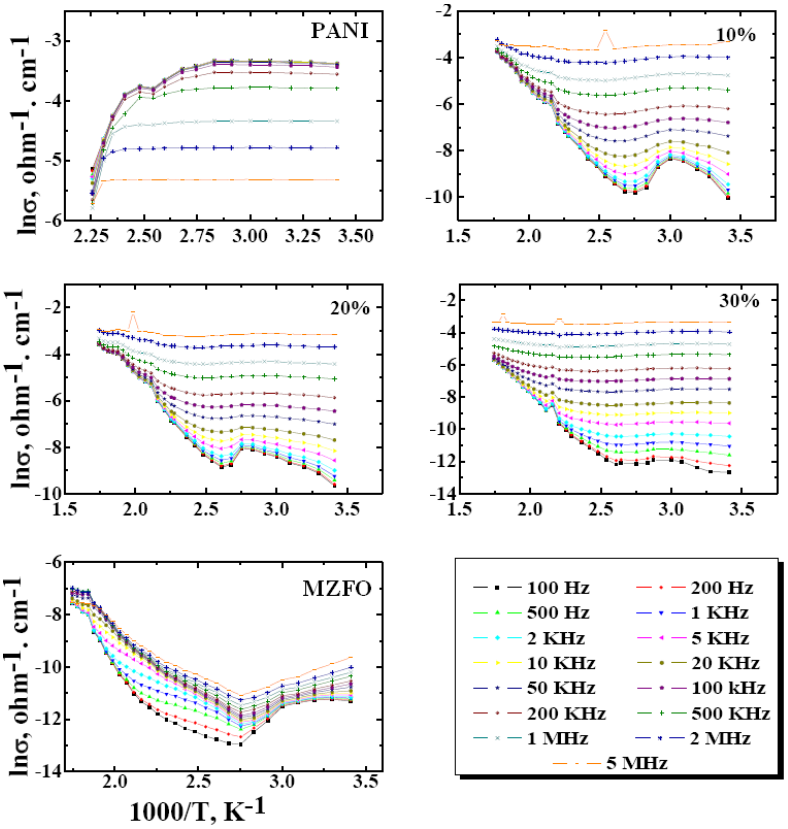

Figure 7. Relation between lnσ and reciprocal of absolute temperature as a function of applied frequency for pure components and PANI/MZFO nano-composites.

The conductivity of pure PANI shows metallic behavior in which conductivity decreases slightly with increasing temperature or frequency. The obvious decrease in conductivity at higher temperatures can be attributed to the predominance of the phonon-electron collision over the mobility effect.

Pure MZFO exhibits a semiconducting behavior in which the conductivity increases with increasing temperature. The metallic like behavior observed at lower temperatures can be due to the insufficient thermal energy (generated at low temperatures) needed to promote electrons to move out of their positions. The slight decrease in the conductivity with increasing temperature (medium temperature region) can be owed to the desorption of water molecules adsorbed on ferrites particles [35].

PANI/MZFO nano-composites with different compositions showed a similar conducting behavior to that of pure MZFO (Fig. 8). The obvious increase in the conductivity values than that of MZFO can be owed to presence of the conducting PANI. In addition, the conductivity values increases with increasing PANI content, which suggests that, the presence of PANI improving the conducting properties of ferrite and indicates the interaction between PANI and MZFO.

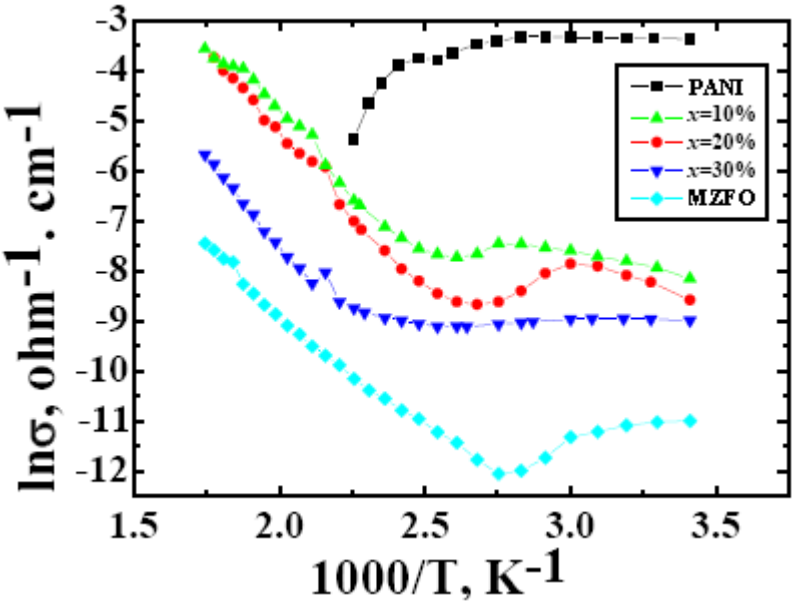

Figure 8. Relation between lnσ and the absolute temperature at an applied frequency of 10 kHz for pure components and PANI/MZFO nano-composites.

4. CONCLUSIONS

Magnetic-conducting polyaniline/$Mn_{0.8}Zn_{0.2}Fe_2O_4$ (PANI/MZFO) nano-composites have been synthesized via in situ polymerization of aniline in the presence of different weight percent of MZFO nano-particles prepared through citrate auto-combustion route. The pure components as well as the composites with different ferrite compositions were characterized using XRD, TG, FT-IR and TEM

techniques. The data analysis showed an interfacial interaction between PANI and MZFO through the formation of core-shell structure and exhibited an increase in the thermal stability of PANI matrix with the addition of MZFO. The magnetic characterization indicated ferromagnetic behavior for MZFO and showed an improvement in the PANI magnetic properties by the addition of MZFO. The conductivity measurements as a function of temperature showed a decrease in the conducting properties of PANI by the addition of MZFO and a consequent change in the electrical properties from metallic to semi-conducting behavior. Generally, the obtained results indicated the possibility of tailoring electromagnetic properties of PANI depending on the weight percent of MZFO.

ACKNOWLEDGEMENT
This paper was funded by the Deanship of Scientific Research (DSR), King Abdulaziz University, Jeddah, under grant No. [135-130-D1432]). The authors therefore, acknowledge with thanks DSR technical and financial support.

References

1. J. Anand, S. Palaniappan, D.N. Sathyanarnayana, *Prog. Polym. Sci.*, 23 (1998) 993.
2. J.C. Aphesteguy, P.G. Bercoff, S.E. Jacobo, *Physica B*, 398 (2007) 200.
3. D.C. Trivedi, In: H.S. Nalwa, editor. Handbook of organic conductive molecule and polymers, vol. 2. Chichester: Wiley (1997) p. 505.
4. R. Ansari, M.B. Keivani, *E-J. Chem.*, 3 (2006) 202.
5. N. Gospodinova, L. Terlemezyan, *Prog. Polym. Sci.*, 23 (1998)1443.
6. A.G. Mac Diarmid, C.J. Chiang, M. Halpern, W.S. Huang, S.L. Mu, N.L.D. Somasiri, W. Wu, S.I. Yaniger, *Mol. Cryst. Liq. Cryst.*, 121 (1985) 173.
7. J. Stejskal, I. Sapurina, *Synth. Met.*, 105 (1999) 195.
8. P. Somani, B.B. Kale, D.P. Amalnerkar, *Synth. Met.*, 106 (1999) 53.
9. M.L. Gautu, P.J.G. Romero, *Sol. State Chem.*, 147 (1999) 601.
10. A.A. Farghali, M. Moussa, M.H. Khedr, *J. Alloys Compds.*, 499 (2010) 98.
11. G.D. Prasanna, H.S. Jayanna, A.R. Lamani, S. Dash, *Synth. Met.*, 161 (2011) 2306.
12. R. M. Khafagy, *J. Alloys Compds.*, 509 9849 (2011).
13. M. Khairy, *Synth. Met.*, 189 (2014) 34.
14. M. Hashim, Alimuddin, S. E. Shirsath, S.S. Meena, R.K. Kotnala, S. Kumar, P. Bhatt, R.B. Jotania, R. Kumar, *Mater. Chem. Phys.*, 141 (2013) 406.
15. C. Wang, Y. Shen, X. Wang, H. Zhang, A. Xie, *Mater. Sci. Semicond. Process.*, 16 (2013) 77.
16. V. Babayan, N.E. Kazantseva, R. Moucka, I. Sapurina, Yu.M. Spivak, V.A. Moshnikov, *J. Magn. Magn. Mater.*, 324 (2012) 161.
17. V. Babayan, N.E. Kazantseva, I. Sapurina, R. Moucka, J.Vilkacova, J. Stejskal, *App. Surf. Sci.*, 258 (2012) 7707.
18. S. Lee, Y. Chen, C. Ho, C. Chang, Y. Hong, *Mater. Sci. Eng. B*, 143 (2007) 1.
19. L. Li, Ch. Xiang, X. Liang, B. Hao, *Synth. Met.*, 160 (2010) 28.
20. J. Jiang, L.-H. Ai, D.-B. Qin, H. Liu, L.-C. Li, *Synth. Met.*, 159 (2009) 695.
21. L.-H. Ai, J. Jiang, *J. Alloys Compd.*, 487 (2009) 735.
22. J. Jiang, L.-H. Ai, *Mater. Lett.*, 62 (2008) 3643.
23. M.A.Gabal, R.S.Al-Luhaibi,Y.M.AlAngari, *Powder Techn.*, 229 (2012) 112.
24. P.K. Roy, J. Bera, *J. Mater. Process. Tech.*, 197 (2008) 279.

25. Reda M. El-Shishtawy, M. Abdel Salam, M.A. Gabal, Abdullah M. Asiri, *Polym. Compos.*, 33 (2012) 532.
26. R.M. Khafagy, *J. Alloys Compd.*, 509 (2011) 9849.
27. C. Leng, J. Wei, Z. Liu, J. Shi, *J. Alloy Compd.*, 509 (2011) 3052.
28. R.T. Ma, H.T. Zhao, G. Zhang, *Mater. Res. Bull.*, 45 (2010) 1064.
29. C.S. Zhang, L. Yang, *J. Magn. Magn. Mater.*, 324 (2012) 1469.
30. R.D. Waldron, *Phys. Rev.*, 99 (1955) 1727.
31. T.H. Ting, R.P. Yu, Y.N. Jau, *Mater. Chem. Phys.*, 126 (2011) 364.
32. S. Sultana, Rafiuddin, M.Z. Khan, K. Umar, *J. Alloys Compd.*, 535 (2012) 44.
33. A. Gok, B. Sari, M. Talu, *Synth. Met.*, 142 (2004) 41.
34. R. Patil, A.S. Roy, K.R. Anilkumar, K.M. Jadhav, S. Ekhelikar, *Composites: Part B*, 43 (2012) 3406.
35. M.A. Gabal1, W.A. Bayoumy, A. Saeed, Y.M. Al Angari, *J. Mol. Struct.*, 1097 (2015) 45.